

Evaluation of the Low-Speed Stability and Control Characteristics of a Mach 5.5 Waverider Concept

David E. Hahne
Langley Research Center • Hampton, Virginia

The use of trademarks or names of manufacturers in this report is for accurate reporting and does not constitute an official endorsement, either expressed or implied, of such products or manufacturers by the National Aeronautics and Space Administration.

Available electronically at the following URL address: <http://techreports.larc.nasa.gov/ltrs/ltrs.html>

Printed copies available from the following:

NASA Center for AeroSpace Information
800 Elkridge Landing Road
Linthicum Heights, MD 21090-2934
(301) 621-0390

National Technical Information Service (NTIS)
5285 Port Royal Road
Springfield, VA 22161-2171
(703) 487-4650

Summary

Static force and moment tests of a 0.062-scale model of a hypersonic vehicle study concept known as the LoFLYTE™¹ configuration were conducted in the Langley 12-Foot Low-Speed Tunnel. These tests looked primarily at the low-speed static stability and control characteristics of this configuration. Data were obtained over an angle-of-attack range of -5° to 22° at sideslip angles that ranged between -10° and 10° . Supporting flow visualization tests were also conducted.

Two primary concerns before the test were whether the configuration had adequate pitch control and adequate directional stability for low-speed operations. The tiperons were sized to provide enough pitch control to trim the vehicle to $\alpha = 16^\circ$ with no more than 10° of surface deflection; however, there still was some concern about achieving this capability. The data obtained in this test showed that 10° of tiperon deflection was nearly sufficient to trim the configuration to the desired angle of attack. Because of the pitching-moment characteristics of the LoFLYTE™ configuration, there is a reasonably high level of unpowered trimmed lift at nominal takeoff and approach to landing angles of attack that should allow for acceptable takeoff and landing speeds for this vehicle.

Initial evaluation of the directional stability characteristics of this configuration showed a significant instability between $\alpha = 10^\circ$ and about $\alpha = 18^\circ$. This test determined that the cause of this instability was the interaction of the wing leading-edge vortex with the vertical tails. Moving the vertical tails either inboard or outboard from the baseline location eliminated this unfavorable interaction. The inboard location, however, is more desirable because it also places the tails in a position where they do not interfere with the tiperons. This location allows for the lower portion of the rudder to be extended (the baseline rudders have a cutout to allow a full 30° of tiperon deflection) and for the vertical tails to be moved farther aft, thus resulting in an additional increase in rudder power.

Introduction

The quest for faster and faster airplanes has been a driving force in aeronautics since the Wright brothers' first flight at the turn of the century. Man has always recognized the military and commercial benefits of decreasing the time it takes to travel between two points, and air travel has always offered the most potential for improvements in the time-distance equation. Efforts to develop a single-stage-to-orbit vehicle during the 1980's rekindled

¹Trademark of Accurate Automation Corporation, Chattanooga, Tennessee.

investigations into airplanes that could travel at hypersonic speeds ($\text{Mach} > 4$). While the X-30 program was expected to leapfrog from vehicles capable of traveling two or three times the speed of sound to velocities in excess of $\text{Mach} 15$, it was understood that the technology for developing a more modest hypersonic vehicle that would travel at five to six times the speed of sound was imbedded in the X-30 program. Advances made in high-temperature materials, lightweight structures, and high thrust-to-weight ratio propulsion systems during the X-30 program have made modest hypersonic vehicles, such as the $\text{Mach} 5.5$ waverider of this study, not only feasible but practical (ref. 1).

Waverider concepts have long been known to be very efficient cruising vehicles in terms of lift-to-drag ratio at their design Mach number (refs. 2 through 4). While these configurations are well suited for operation at design conditions, flying characteristics for off-design conditions, particularly at low speed, can become undesirable. The waverider-derived configuration of the present study is optimized for a Mach number of 5.5 (ref. 1), and as with all configurations designed for hypersonic flight, it incorporates many highly swept surfaces. Both the wing and the vertical tail of this configuration are swept to 75° . The vortical flows that dominate the aerodynamics of such highly swept surfaces can result in complex and quickly changing flying characteristics at low-speed conditions. The present investigation was intended to document the low-speed aerodynamic characteristics of this configuration, with emphasis on static stability and control, and to understand the complex vortical interactions that dominate these characteristics.

Symbols

All data initially were obtained in the body-axis system. Longitudinal forces and moments are presented in the stability-axis system, and lateral-directional forces and moments are presented in the body-axis system. All aerodynamic moments were computed about a center-of-gravity location of 58 percent of the body length measured from the nose of the fuselage.

b	wing span, ft
C_L	lift coefficient, $\frac{\text{Lift}}{\bar{q}S}$
C_l	rolling-moment coefficient, $\frac{\text{Rolling moment}}{\bar{q}Sb}$
C_m	pitching-moment coefficient, $\frac{\text{Pitching moment}}{\bar{q}Sl}$
C_n	yawing-moment coefficient, $\frac{\text{Yawing moment}}{\bar{q}Sb}$

C_Y	side-force coefficient, $\frac{\text{Side force}}{\bar{q}S}$
I_x, I_y, I_z	body axes moments of inertia, slugs-ft ²
L/D	lift-to-drag ratio
l	body length, ft
p	body axes roll rate, rad/sec
p_s	stability axes roll rate, rad/sec
\dot{p}	roll-rate acceleration, rad/sec ²
\dot{q}	pitch-rate acceleration, rad/sec ²
\bar{q}	free-stream dynamic pressure, lb/ft ²
r	body axes yaw rate, rad/sec
\dot{r}	yaw rate acceleration, rad/sec ²
S	wing-body planform area, ft ²
V	free-stream velocity, knots
W	vehicle weight, lb
X, Y, Z	body axes
α	angle of attack, deg
β	angle of sideslip, deg
ΔC_l	incremental rolling-moment coefficient
ΔC_m	incremental pitching-moment coefficient
ΔC_n	incremental yawing-moment coefficient
ΔC_Y	incremental side-force coefficient
δ_t	tiperon deflection, positive trailing edge down, deg
δ_r	rudder deflection, positive trailing edge left, deg

Stability derivatives:

$$C_{l_\beta} = \frac{\partial C_l}{\partial \beta} \quad C_{n_\beta} = \frac{\partial C_n}{\partial \beta} \quad C_{Y_\beta} = \frac{\partial C_Y}{\partial \beta}$$

$$C_{l_{\delta_r}} = \frac{\partial C_l}{\partial \delta_r} \quad C_{n_{\delta_r}} = \frac{\partial C_n}{\partial \delta_r}$$

$$C_{l_{\delta_t}} = \frac{\partial C_l}{\partial \delta_t} \quad C_{n_{\delta_t}} = \frac{\partial C_n}{\partial \delta_t}$$

Subscripts:

app	approach
o	value at zero angle of attack
TO	takeoff

tr	trimmed value ($C_m = 0$)
xw	crosswind

Abbreviations:

BW	body with blended wing
L	left
N	engine nacelle
R	right
V	vertical tails
WL	waterline, in.

Model

The configuration tested is a 0.062-scale model of a hypersonic vehicle study concept called LoFLYTE™ (fig. 1). The configuration consists of blended wing-body, twin wing-mounted vertical tails, and an engine nacelle package located on the underside of the body. The model, 8.34 ft long with a 5.19-ft wing span, has an initial leading-edge sweep of 75.13°, which changes to 65° along the leading edge of the tiperons. The tiperons, deflectable wingtips that also incorporate a more conventional trailing-edge surface, are used for both pitch and roll control. Each vertical tail has a leading-edge sweep of 75° and a full-height rudder with an aft-swept hing line of 26.6°. The baseline rudders have a cutout, or notch, at the bottom to allow a full 30° of tiperon deflection. In addition to the baseline position (fig. 1(a)), four alternate vertical tail locations were tested: (1) 8 in. outboard of the baseline location, (2) 4 in. inboard of the baseline location, (3) a single centerline vertical tail, and (4) 4 in. inboard and 4 in. aft of the baseline location. For the fourth alternate vertical tail location, the notch in the rudder was filled. The engine nacelle was a simple flow-through shell attached to the underside of the body. Geometric details of the model are given in table I.

Tests

A photograph of the model and test setup is shown in figure 2. Tests were conducted in the Langley 12-Foot Low-Speed Tunnel at a dynamic pressure of 4 lb/ft². This dynamic pressure corresponds to a Reynolds number of 3.08×10^6 based on body length. Force and moment coefficients were obtained over an angle-of-attack range between -5° and 22° at sideslip angles of 0°, -4°, and 4°. Data obtained at sideslip angles of -4° and 4° were used to compute lateral-directional derivatives. Data were also obtained for some configurations over a sideslip angle range from -10° to 10° at selected angles of attack. Forces and moments were measured on an internal six-component strain-gauge balance. Standard corrections for wall interference and blockage, as described in

reference 5, as well as flow angularity corrections, were applied to the data. Although comparison with data obtained on the baseline configuration in the Langley 30-by 60-Foot Tunnel showed good agreement with the present test, studies have shown the potential for the model support system and the tunnel drive system to affect the breakdown of vortex flows over the model. Limited laser light-sheet flow visualization studies, although not shown, were also conducted to help interpret the force and moment data.

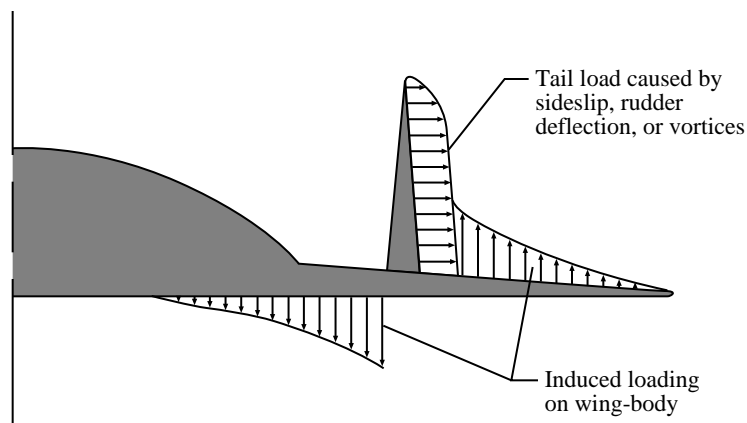
Results

Longitudinal Characteristics

The effect of the configuration components on the longitudinal aerodynamic characteristics of the model are shown in figure 3. For the body-wing (BW) and the body-wing-nacelle (BWN) configurations, the influence of a strong leading-edge vortex can be seen in both the lift and pitching-moment coefficients. In lift, this influence can be seen as a continuous increase in the lift-curve slope with increasing angle of attack above $\alpha = 4^\circ$. The effect on pitching moment is seen as a mild pitch-up that begins near the same angle of attack. Below $\alpha = 8^\circ$, both the tail-off (BW and BWN) and tail-on (BWV and BWNV) configurations have similar longitudinal characteristics. It is clear from both the force and moment data in figure 3 that the vertical tails interact with the leading-edge vortex system. This interaction is evidenced by the decrease in the lift-curve slope seen for the tail-on configurations at angles of attack above 8° and by distinct changes in pitch stability between $\alpha = 11^\circ$ and $\alpha = 15^\circ$. Flow visualization studies also showed that the path of the leading-edge vortex was very close to the baseline vertical tail location. While the decrease in lift-curve slope was expected, the behavior in pitch was not typical for wing-mounted vertical tails on this type of configura-

tion. Normally, wing-mounted vertical tails will cause the leading-edge vortex to burst prematurely, resulting in a severe pitch-up. For this configuration, however, addition of the vertical tails results in an increase in pitch stability before the unstable pitch-up. The reason for this behavior is not fully understood, but is believed to result from the load induced on the wing that is produced from the interaction of the wing leading-edge vortices with the vertical tails. Based on the span loading data presented in reference 6, and illustrated in sketch A, the following argument can be made: side loads on the vertical tails that are produced by the wing leading-edge vortices induce an upward load on the wing outboard of the vertical tails and a downward load on the wing inboard. Normally the downward load and the upward load would balance out; however, because of the presence of the fuselage, part of the downward load is directed laterally. The result is a net upload which produces the pitch-down moment seen in figure 3. Above $\alpha = 15^\circ$, the side load produced by the leading-edge vortices decreases as the vortices move farther from the vertical tails, and the pitching-moment curve again becomes unstable.

The effectiveness of the tiperons for providing pitch control is presented in figure 4. The tiperons were sized to provide enough pitch control to trim the vehicle to $\alpha = 16^\circ$ with no more than 10° of surface deflection; however, there still was some concern about achieving this capability. As can be seen from the data, this goal was nearly achieved, as 12° of tiperon deflection is sufficient to trim the configuration to the desired angle of attack. Tiperon effectiveness does decrease for deflections above 12° , however, and this reduced effectiveness may be a concern in generating sufficient nose-down pitch rates for recovery from angles of attack beyond 15° . An analysis using representative weights and inertias for this type of vehicle (using approach-to-landing conditions) was therefore made to determine the



Sketch A

nosedown pitch-control requirements. Inertia values for the Space Shuttle orbiter (ref. 7) were used for this and other analyses as the orbiter's weight and size are reasonably close to the LoFLYTE™ configuration's landing configuration. Unless otherwise noted, the analyses presented in this report are based on the values listed in table II.

The pitch-control analysis used the criteria discussed in references 8 and 9 for relaxed pitch-stability configurations to determine the required level of nose-down pitching moment for satisfactory recovery response. The level of nose-down pitching moment required C_m^* at a given angle of attack is

$$C_m^* = \frac{I_y \dot{q}}{\bar{q} S l}$$

where the value of \dot{q} is -0.08 rad/sec^2 . While this criterion was initially developed for stall and poststall angles of attack, the pitch-rate acceleration requirement for Mil-Spec class III vehicles (non-high-performance aircraft) is also applicable to noncritical pitch maneuvers at all angles of attack. The analysis was made for a trimmed condition at $\alpha = 15^\circ$ ($C_L = 0.6$). The available nose-down $\Delta C_m = -0.022$ (fig. 4). Based on the equation above, $C_m^* = -0.011$ for landing weight. This result indicates that the present configuration would have satisfactory nose-down recovery characteristics in terms of handling qualities.

Figure 5 shows the trimmed values of C_L and L/D as well as the tiperon deflection required for trim that is based on the results shown in figure 4. Because of the pitching-moment characteristics of this configuration (neutral to unstable static margin and positive $C_{m,0}$), the vehicle has a reasonably high level of unpowered trimmed C_L at nominal takeoff and approach-to-landing conditions ($\alpha = 10^\circ$). As a result, takeoff speeds of 263 knots are possible at full gross weight (551 052 lb). If the lift component of thrust and the expected nose-up pitching moment caused by thrust were to be accounted for, the takeoff speed would be significantly less than 263 knots. For approach-to-landing conditions, the approach speed for a nominal weight of 183 000 lb would be 151 knots. While this speed is somewhat high when compared with some conventional aircraft, it is a very reasonable speed for this vehicle class. (Shuttle orbiter landing speeds are in excess of 200 knots.)

Lateral-Directional Characteristics

The effect of the configuration components on lateral-directional aerodynamic characteristics is presented in figure 6. As would be expected for a configuration with such a highly swept planform, the level of lateral stability increases with angle of attack to quite

high values. These high levels of lateral stability may have an adverse impact on landing operations in cross-wind conditions. As can be seen at angles of attack above $\alpha = 14^\circ$, adding the vertical tails reduced lateral stability. Flow visualization studies indicated that at angles of attack near 14° the windward leading-edge vortex has moved very close to the outboard side of the windward vertical tail. At the same time, the leeward vortex has moved farther outboard but is still in proximity to the wing upper surface. The side load generated on the windward vertical tail by the windward vortex, acting above the center of gravity of the configuration, and the upload on the wing outer panel generated by the leeward vortex would tend to reduce lateral stability. As angle of attack is increased, the vertical tails tend to force the leading-edge vortices to burst over the wing, which reduces lateral stability even further.

Without the vertical tails, the configuration, as expected, was unstable directionally up to about $\alpha = 10^\circ$. Above these angles of attack, the wing-body exhibits stable values of C_{n_β} that appear to be caused by forces aft of the center of gravity (C_{Y_β} is increasingly negative).

This type of behavior is usually associated with forebody vortical flows, although these usually produce forces on the forebody. Addition of the vertical tails generates a stable increment that results in stable directional characteristics up to $\alpha = 10^\circ$. Between $\alpha = 10^\circ$ and $\alpha = 18^\circ$, the vertical tails decrease the stability of the configuration below that of the wing-body alone. It is not unusual for the interaction of the wing leading-edge vortex and the vertical tails to produce these directional characteristics. Beyond $\alpha = 18^\circ$, it appears that the wing-body directional-stability characteristics dominate the aerodynamics.

Figure 7 presents the effectiveness of the tiperons for providing roll control. The tiperons, deflected asymmetrically, do generate significant rolling moment, and the control effectiveness is fairly linear (that is, the change in moment versus control deflection is a linear function). Up to $\alpha = 10^\circ$, the levels of adverse yawing moment generated by the tiperons are independent of control deflections above $\pm 12^\circ$. Beyond $\alpha = 10^\circ$, only the largest deflections increase adverse yawing moments significantly. These relatively large values for yawing moment caused by roll control are believed to be a result of an induced sidewash at the vertical tails. As theorized, this sidewash results from flow curling around the inboard portion of the wing along the streamwise cut between the wing and the tiperons and generates a positive sideslip at the vertical tails for a right roll-control input.

In general, the levels of roll control would appear to be adequate; however, because of the high levels of static

lateral stability, a crosswind analysis, to be discussed later in this section, must be performed. This analysis also will require the rudder effectiveness data presented in figure 8. Like the tiperons, rudder effectiveness appears to be linear with control deflection. As would be expected, rudder power does decrease as angle of attack is increased beyond about 8°. This reduction may be a result of the large wing-body planform shielding the vertical tails and effectively reducing the dynamic pressure at the rudders. It is more likely, however, the result of a more complex interaction of the wing leading-edge vortices with the vertical tails, which are heavily loaded because of rudder deflection. In this situation the leading-edge vortices are forced into an asymmetric position relative to the vertical tails, with the port side leading-edge vortex having the stronger influence for positive rudder deflections. This vortex arrangement produces an incremental load on the vertical tails that opposes that caused by rudder deflection. Unlike the tiperons, however, deflection of the twin rudders produces a favorable cross derivative (rolling moment caused by rudder deflection) for angles of attack below $\alpha = 13^\circ$. The flow physics here are similar to those discussed previously in the Longitudinal Characteristics section in relation to the stabilizing effect the vertical tails had on pitching moment. (See sketch A.) In this case the side loads on the vertical tail that are caused by positive rudder deflection result in an induced wing loading that produces a negative increment to rolling moment. Because the wing is so large, this increment is greater than the positive rolling moment produced by forces on the vertical tail. The net result is a configuration with proverse rolling moment caused by rudder deflection. Consequently, rudder inputs will tend to be self-coordinating and will require less asymmetric tiperon deflection to make a coordinated turn. As will be discussed later in this section, this self-coordination will have a positive impact on the crosswind capabilities of this configuration because of the high levels of adverse yaw generated by the tiperons.

Because approach to landing probably will be the most demanding low-speed flight phase for this vehicle, the conditions chosen for the crosswind and coordinated roll analyses were as follows: $\alpha = 10^\circ$, $V = 151$ knots, $W = 183\,000$ lb. The crosswind analysis involves solving the following set of simultaneous algebraic equations for δ_t and δ_r :

$$C_{n_\beta} \beta + C_{n_{\delta_t}} \delta_t + C_{n_{\delta_r}} \delta_r = 0$$

$$C_{l_\beta} \beta + C_{l_{\delta_t}} \delta_t + C_{l_{\delta_r}} \delta_r = 0$$

where $\beta = \tan^{-1} \frac{V_{xw}}{V_{app}}$.

The solution for these equations is shown in figure 9 for $\alpha = 10^\circ$. In general, this type of vehicle must demonstrate the ability to land in a 30-knot crosswind. To trim out the sideslip generated by this crosswind and to align the vehicle with the runway centerline would require 22° of asymmetric tiperon and 13° of rudder deflection (by using control derivatives based on full-control deflection). Because of the high levels of adverse yaw generated by the tiperons, both the rudders and the tiperons are deflected positively for negative sideslip angles (trimming at sideslip usually requires the vehicle to be cross controlled). Obviously, the rudder requirement is reasonable, as only half the available control authority is used. The tiperon requirement, however, is more severe. When combined with the necessary symmetric tiperon deflection for pitch trim (which reduces the available asymmetric deflection to 25°), one of the tiperons always will be deflected nearly to its limits at these conditions. These levels of control deflections will greatly reduce the nose-down pitch and roll-control margins available for maneuvering and stability augmentation. A reduction in lateral stability or nonzero sideslip approaches are two potential solutions to this problem.

While the ability to make a velocity vector roll in this vehicle may not be mandatory, it is desirable and the associated analysis does provide an indication of the relative balance between roll and yaw control. By using the vehicle equations of motion, it is possible to develop a relationship between roll and yaw control so that a rolling maneuver can be made without generating any sideslip. Like the nose-down pitch-control analysis presented earlier, this analysis requires knowing the moments of inertia of the vehicle. As noted before, inertia values have been estimated by using the Shuttle orbiter data. Starting with the kinematic relation between a stability axis roll rate (with no yaw rate in the stability axes) and the body axes roll and yaw rates,

$$p = p_s \cos \alpha$$

$$r = p_s \sin \alpha$$

and the relationship between rate acceleration and control moments,

$$\dot{p} = \frac{C_{l_{\delta_t}} \delta_t \bar{q} S b}{I_x}$$

$$\dot{r} = \frac{C_{n_{\delta_r}} \delta_r \bar{q} S b}{I_z}$$

an approximate relationship between rudder and asymmetric tiperon deflection for a velocity vector roll can be developed when angle of attack is assumed to remain constant. This relationship is

$$\frac{\delta_r}{\delta_t} \approx \left(\frac{C_{l_{\delta_t}}}{C_{n_{\delta_r}}} \right) \left(\frac{I_z}{I_x} \right) \tan \alpha$$

This simplified analysis indicates that for roll maneuvers at $\alpha = 10^\circ$, 6.4° of rudder deflection would be needed for every 1° of asymmetric tiperon deflection. With a rudder deflection limit of 30° , this would mean that a velocity vector roll would be possible only for asymmetric tiperon deflections of less than 5° . As a result, if larger roll rates are desirable, a way to improve rudder power must be found. It should be noted, however, that this analysis does not account for damping caused by velocity vector roll rate. If the damping terms are large, this analysis is only valid for the initiation of the rolling maneuver.

Alternate Vertical Tail Configurations

In order to address the two directional stability and control problem areas of poor rudder power and directional instability between $\alpha = 10^\circ$ and $\alpha = 18^\circ$, alternate locations for the vertical tails were investigated. Four additional geometries were evaluated: (1) 8 in. outboard of the baseline location, (2) 4 in. inboard of the baseline location, (3) a single centerline vertical tail, and (4) 4 in. inboard and 4 in. aft of the baseline location. The aerodynamic characteristics for the first three configurations are compared to the baseline tails in figure 10. Alternate tail locations had little impact on longitudinal characteristics below $\alpha = 10^\circ$ (fig. 10(a)). Above this angle of attack, changes in both lift and pitching moment are indicative of changes in the way the vertical tail interacts with the wing leading-edge vortex system. The outboard tail location apparently causes the leading-edge vortex to burst, which results in a pitch-up and in a reduction in the lift-curve slope. Flow visualization studies showed no vortex bursting for the inboard tail location although the behavior of the longitudinal data does show some pitch-up when compared with the centerline tail.

As can be seen in both the lateral and directional data (fig. 10(b)), all three alternate geometries eliminated the adverse interaction between the wing leading-edge vortex and the vertical tails. While the outboard location provided the largest stabilizing increment, the level of directional stability associated with the inboard twin-tail location is adequate for this vehicle. The inboard location also allows for the tails to be moved farther aft and eliminates any potential physical interference problem between the rudder and the tiperons, thus allowing the notch in the baseline rudder to be filled. The effect of the alternate tail locations on rudder power is presented in figure 10(c). The results of the alternate twin-tail loca-

tions are mixed and indicate the complex nature of the interaction between the wing leading-edge vortex system and the vertical tails. Rudder power for the centerline tail, while well behaved, is greatly reduced because of the decrease in rudder volume for this configuration. This reduced rudder power is not surprising because the centerline tail was the same geometry as one of the baseline twin tails.

Figure 11(a) shows that moving the tails aft had only a slight effect on lateral-directional stability, namely, by providing a small increase in the level of directional stability. Note that the aft tail data were obtained with the rudder notch filled. There was, however, a significant increase in the effectiveness of the rudders for the aft tail location. Figure 11(b) compares the available rudder power for the forward and aft tail positions. Moving the tails aft and filling the rudder notch resulted in close to a 50-percent increase in rudder power. This increase would allow velocity vector rolls with up to 8° of asymmetric tiperon deflection. While this increase is small, it may make the rolling performance of the LoFLYTE™ vehicle more acceptable.

Concluding Remarks

In general, the low-speed characteristics of the LoFLYTE™ configuration (Accurate Automation Corporation, Chattanooga, Tennessee) appear satisfactory. Because of the pitching-moment characteristics of this configuration (neutral to unstable static margin and positive $C_{m,0}$), the vehicle has a reasonably high level of unpowered trimmed C_L at nominal takeoff and approach-to-landing conditions ($\alpha = 10^\circ$). These levels of unpowered trimmed C_L should allow for acceptable takeoff and landing speeds for this vehicle. Locating the vertical tails inboard of the baseline location improved a directional-stability problem between $\alpha = 10^\circ$ and $\alpha = 18^\circ$. Lateral-directional stability and control characteristics are such that crosswind and velocity vector roll criteria can be met, although control saturation remains an issue in both cases. Reduction in static lateral stability or a modified approach-to-landing profile (i.e., a nonzero sideslip approach) would alleviate the saturation problem during crosswind landings. Higher levels of yaw control are necessary to address the issue of velocity vector rolls. Moving the vertical tails inboard and aft of the baseline location does improve rudder power; however, the increase in the roll-rate envelope is small.

NASA Langley Research Center
Hampton, VA 23681-0001
January 8, 1997

References

1. Pegg, Robert J.; Hunt, James L.; Petley, Dennis H.; Burkhardt, Leo; Stevens, Daniel R.; Moses, Paul L.; Pinckney, S. Z.; Kabis, Hane Z.; Spoth, Kevin A.; and Dziedzic, William M.: Design of a Hypersonic Waverider-Derived Airplane. AIAA-93-0401, Jan. 1993.
2. Townend, L. H.: Research and Design for Lifting Reentry. *Prog. Aerosp. Sci.*, vol. 19, 1979, pp. 1–80.
3. Capriotti, Diego; Bowcutt, Kevin G.; and Anderson, John D., Jr.: Viscous Optimized Hypersonic Waveriders. AIAA-87-0272, Jan. 1987.
4. Anderson, John D., Jr.; Lewis, Mark J.; and Corda, Stephen: Several Families of Viscous Optimized Waveriders—A Review of Waverider Research at the University of Maryland. *Proceedings of the 1st International Hypersonic Waverider Symposium*, Univ. of Maryland, Oct. 1990, p. 39.
5. Pope, Alan; and Harper, John J.: *Low-Speed Wind Tunnel Testing*. John Wiley & Sons, 1966.
6. Queijo, M. J.; and Riley, Donald R.: *Calculated Subsonic Span Loads and Resulting Stability Derivatives of Unswept and 45° Sweptback Tail Surfaces in Sideslip and in Steady Roll*. NACA TN 3245, 1954.
7. Boyden, R. P.; and Freeman, D. C., Jr.: *Subsonic and Transonic Dynamic Stability Characteristics of a Space Shuttle Orbiter*. NASA TN D-8042, 1975.
8. Nguyen, Luat T.; and Foster, John V.: *Development of a Preliminary High-Angle-of-Attack Nose-Down Pitch Control Requirement for High-Performance Aircraft*. NASA TM-101684, 1990.
9. Ogburn, Marilyn E.; Foster, John V.; Pahle, Joseph W.; Wilson, R. J.; and Lackey, James B.: Status of the Validation of High-Angle-of-Attack Nose-Down Pitch Control Margin Design Guidelines. AIAA-93-3623, Aug. 1993.

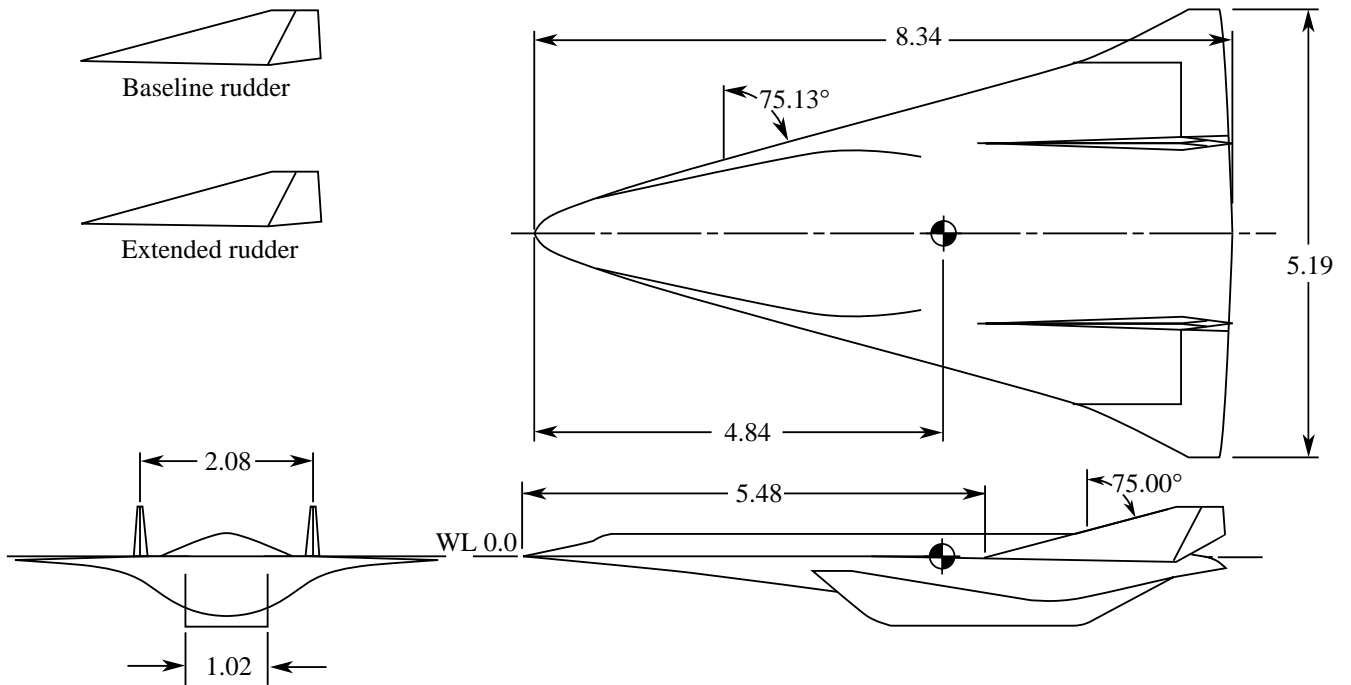
Table I. Geometric Characteristics of LoFLYTE™ Model

Overall length, ft	8.34
Wing-body:	
Span, ft	5.19
Area, ft ²	22.62
Reference length, ft	8.34
Aspect ratio	1.19
Tip chord, ft	0.48
Inboard leading-edge sweep, deg	75.13
Outboard leading-edge sweep, deg	65.00
Trailing-edge sweep, deg	-5.00
Tiperon area (each), ft ²	1.14
Baseline twin vertical tail:	
Span, ft	0.59
Area (each), ft ²	0.87
Root chord, ft	2.86
Aspect ratio	0.40
Leading-edge sweep, deg	75.00
Rudder area (each), ft ²	0.14
Twin vertical tail with extended rudder:	
Span, ft	0.59
Area (each), ft ²	1.03
Root chord, ft	2.86
Aspect ratio	0.34
Leading-edge sweep, deg	75.00
Rudder area (each), ft ²	0.30
Centerline vertical tail:	
Span, ft	0.59
Area (each), ft ²	0.87
Root chord, ft	2.86
Aspect ratio	0.40
Leading-edge sweep, deg	75.00
Rudder area (each), ft ²	0.14

Table II. Data Used for Analytical Calculations

[Data for trimmed conditions at $\alpha = 10^\circ$; inertias are for landing weight of 183 000 lb]

W_{TO} , lb	551 052
W_{landing} , lb	183 000
I_x , slugs-ft ²	747 424
I_y , slugs-ft ²	5 682 812
I_z , slugs-ft ²	5 800 737
S , ft ²	5884
b , ft	83.7
l , ft	134.5
C_L	0.38
L/D	3.9
δ_t , deg	5.5
C_{n_β} , per deg	.00015
C_{l_β} , per deg	-.003
$C_{n_{\delta_t}}$, per deg	.00027
$C_{l_{\delta_t}}$, per deg	-.0015
$C_{n_{\delta_r}}$, per deg	-.00032
$C_{l_{\delta_r}}$, per deg	-.00003



(a) Three-view sketch of model.



(b) Photograph of LoFLYTE™ model.

Figure 1. Test configuration. All dimensions in feet unless otherwise noted.



Figure 2. Photograph of test setup in Langley 12-Foot Low-Speed Tunnel.

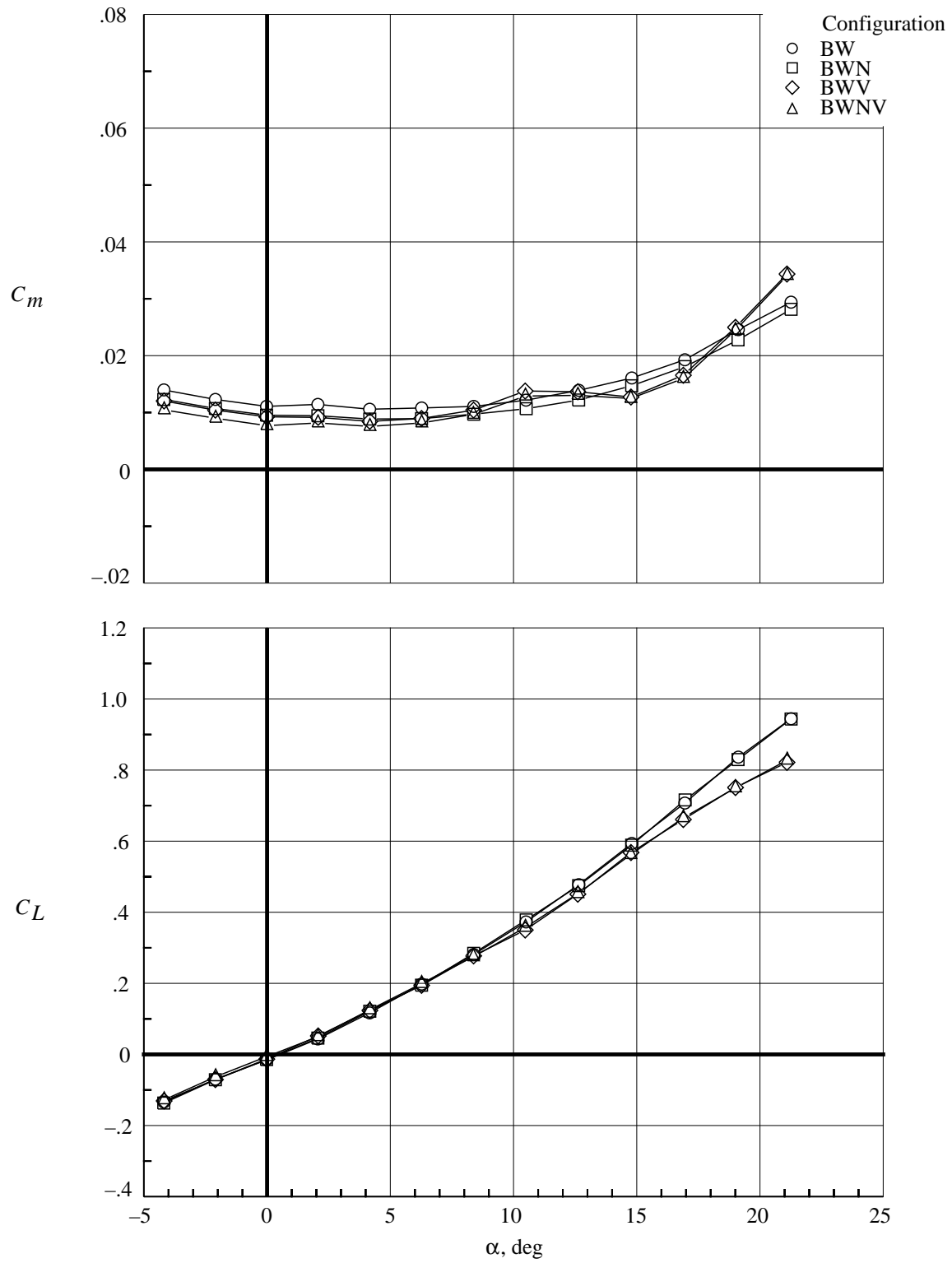


Figure 3. Longitudinal characteristics of test configuration.

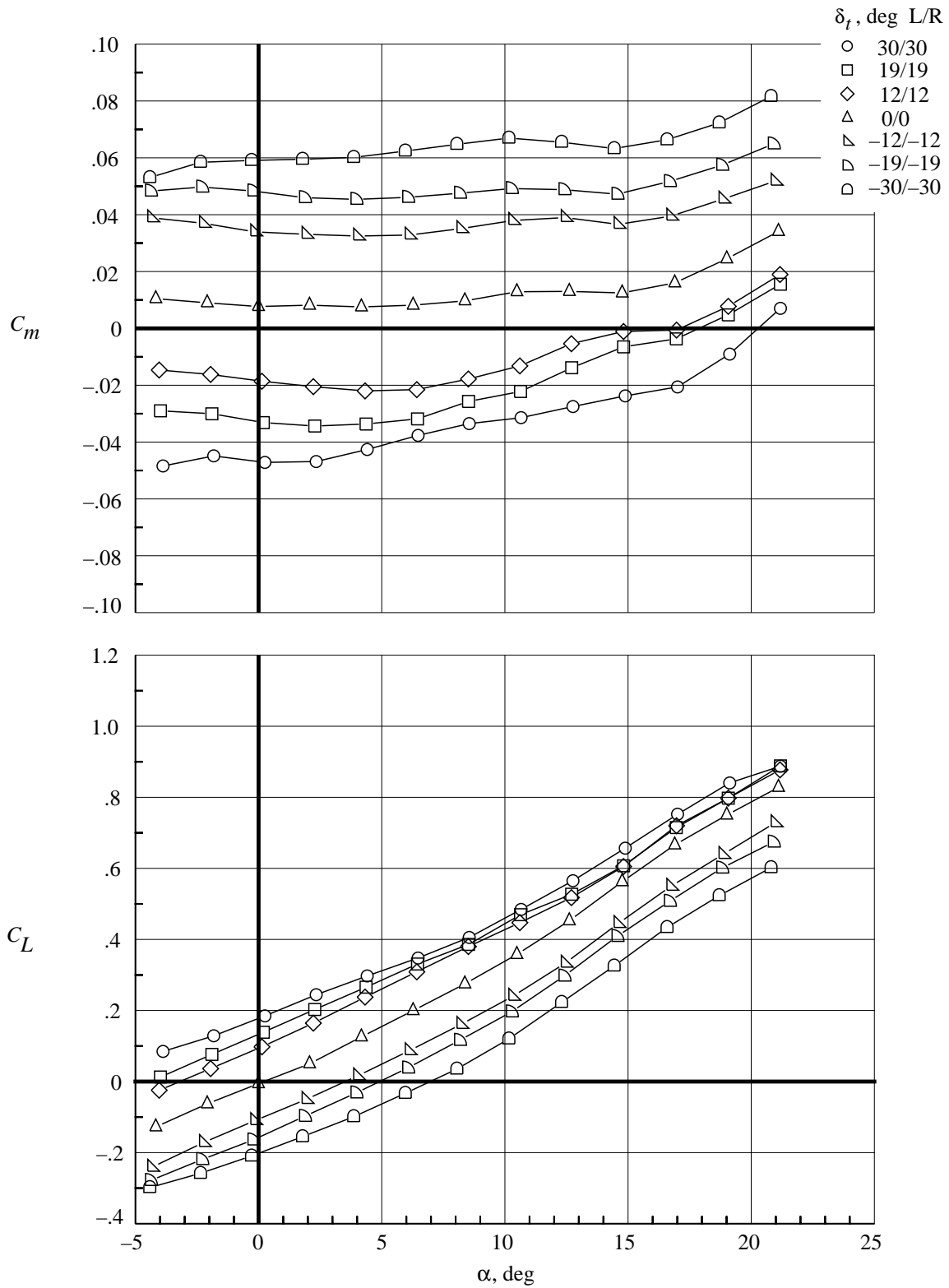


Figure 4. Pitch-control effectiveness.

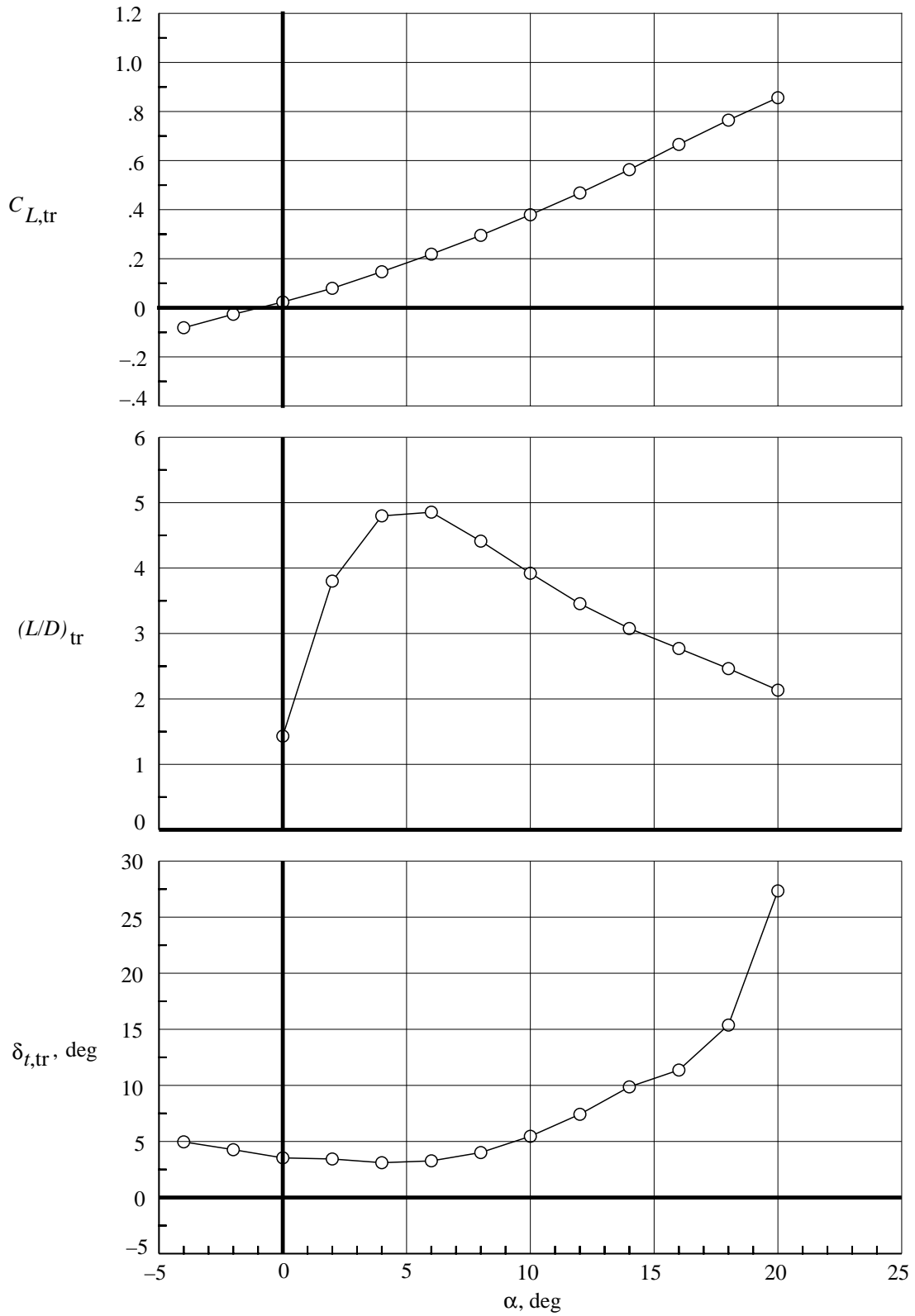


Figure 5. Trimmed longitudinal characteristics.

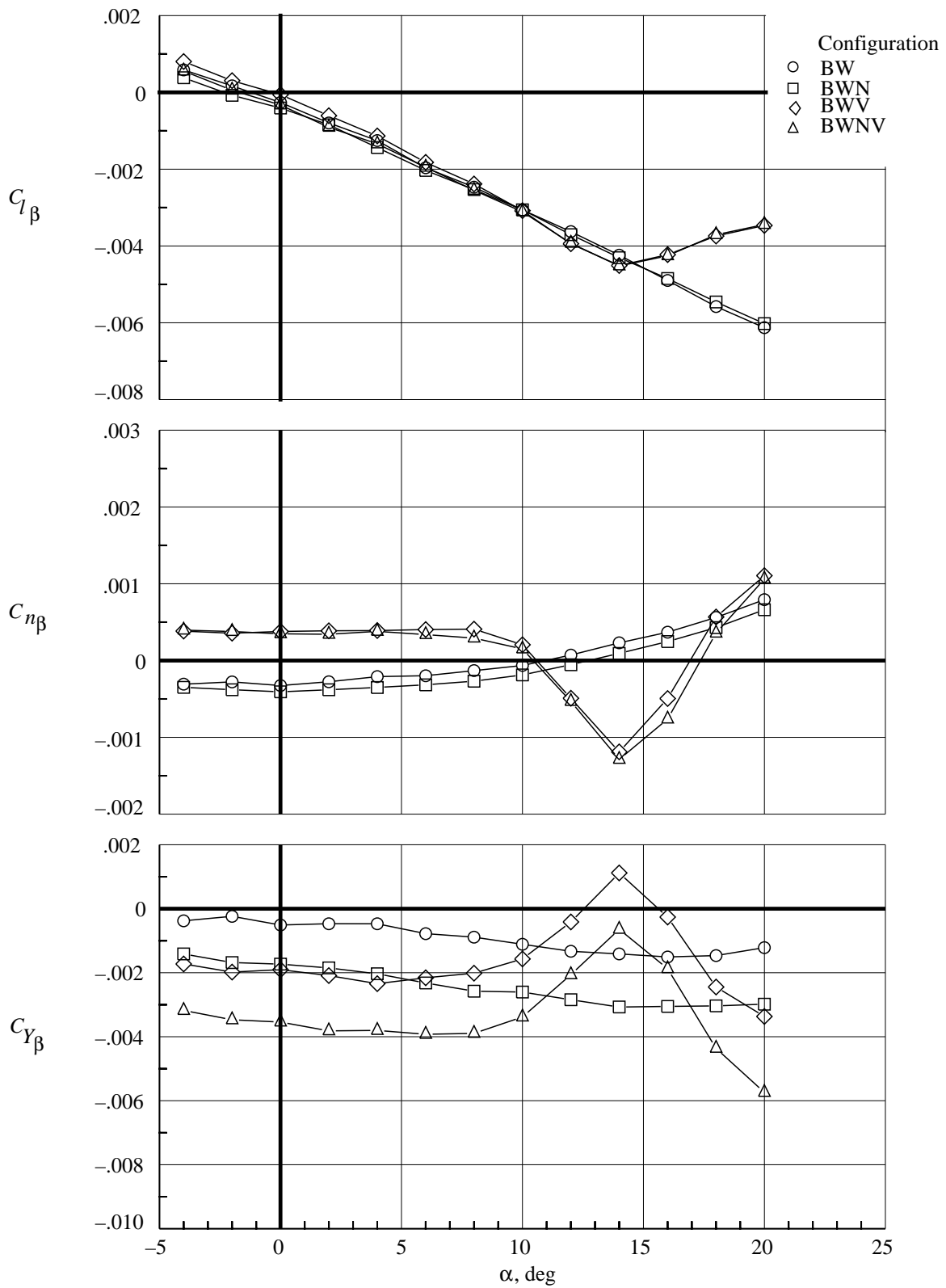


Figure 6. Lateral-directional characteristics of test configuration.

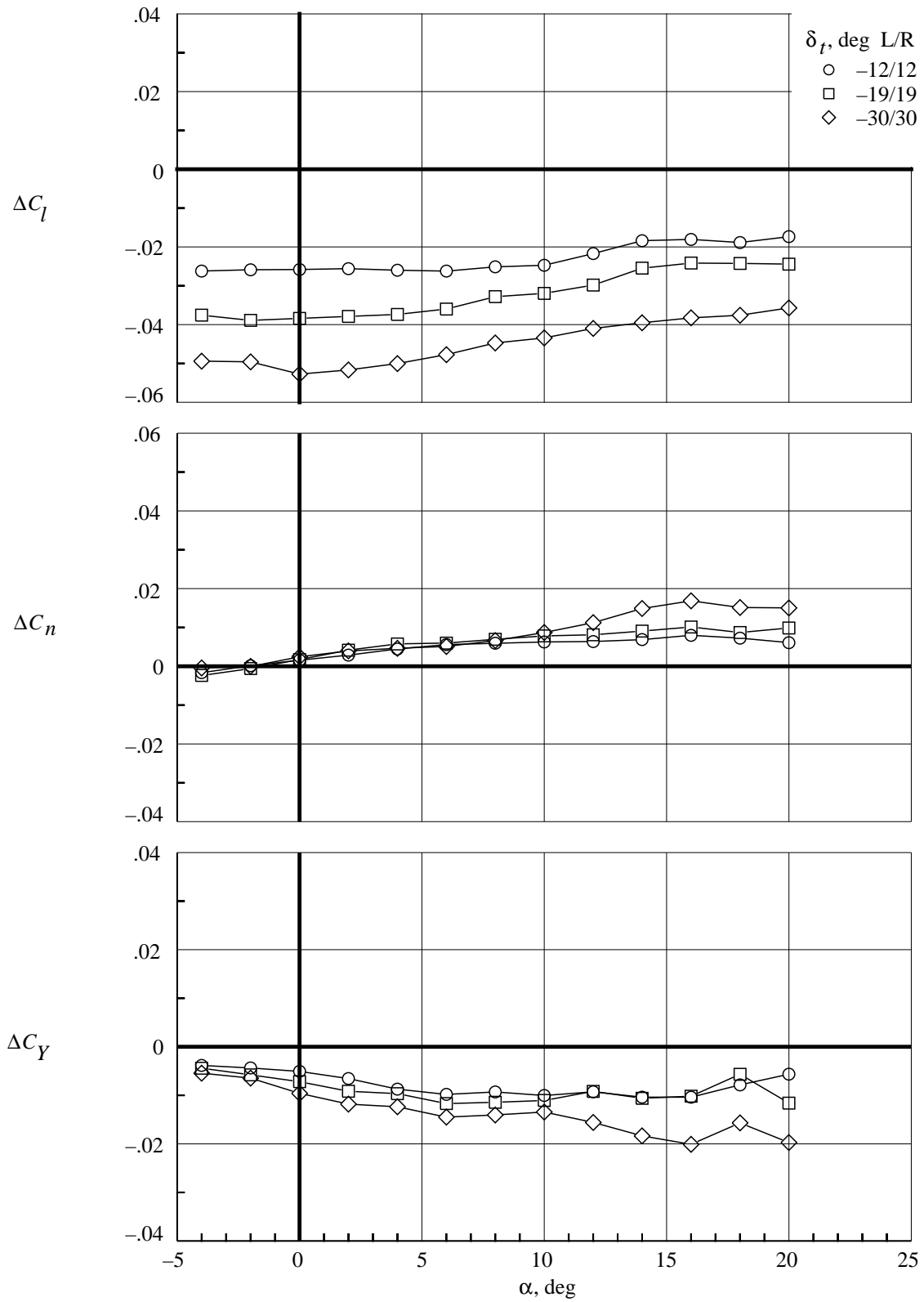


Figure 7. Roll-control effectiveness.

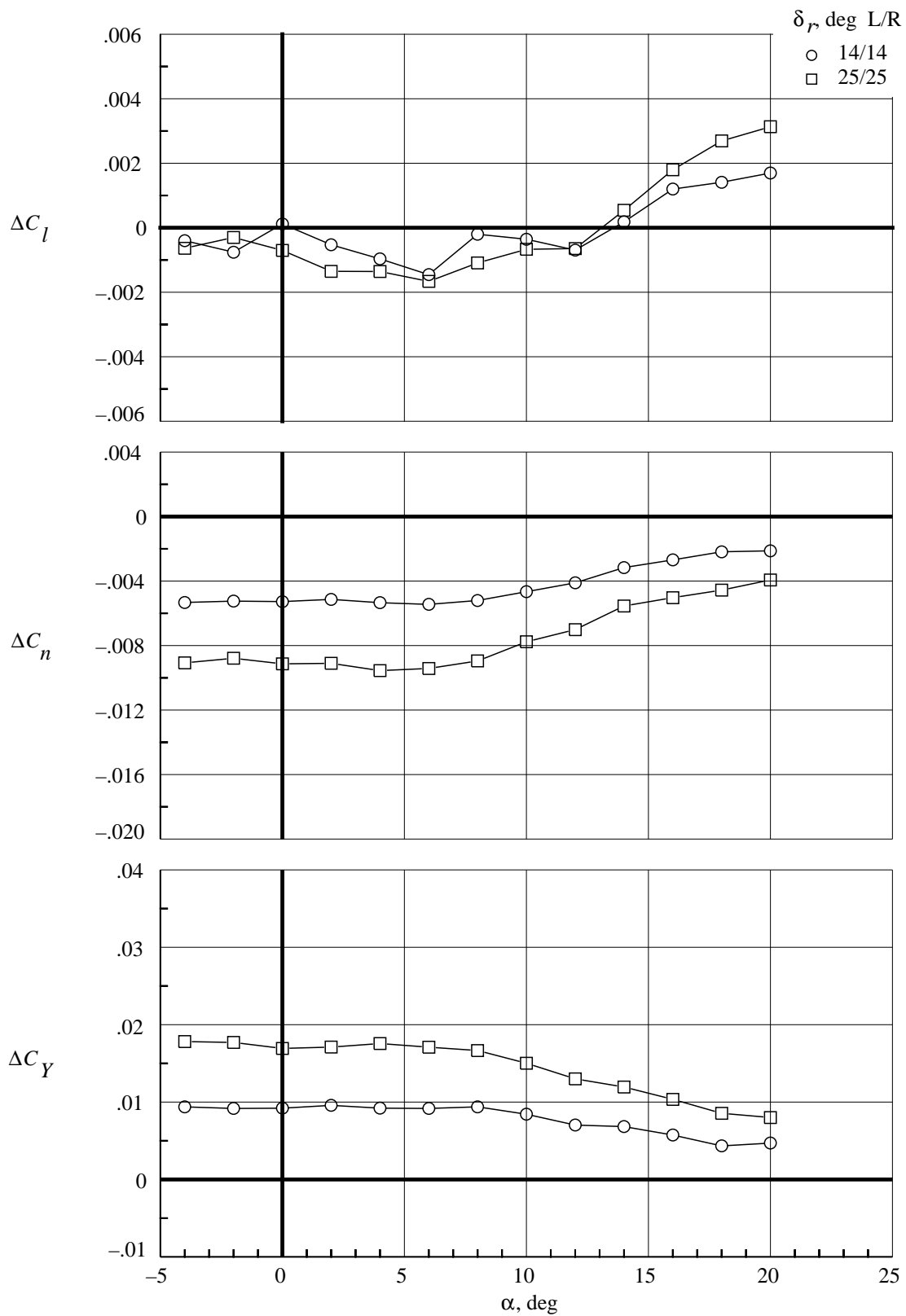


Figure 8. Rudder effectiveness.

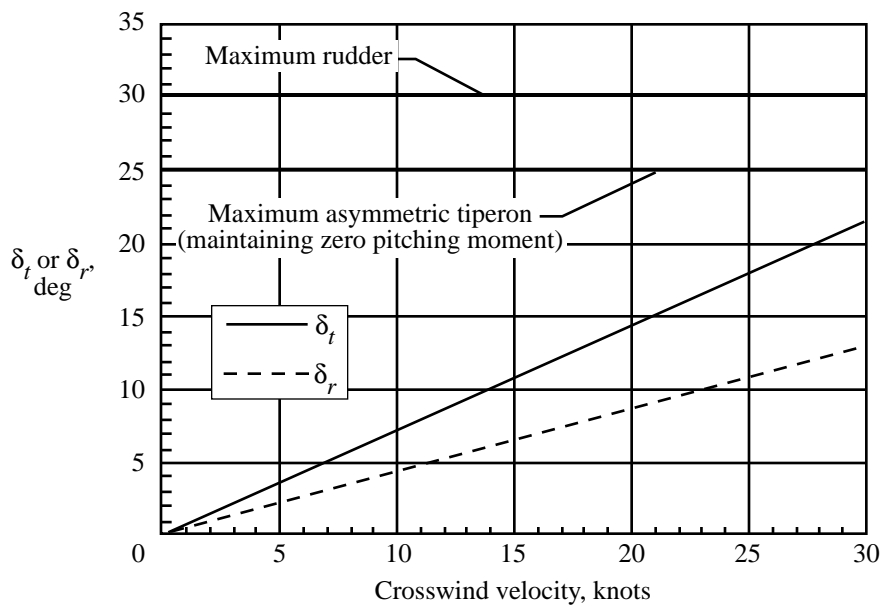
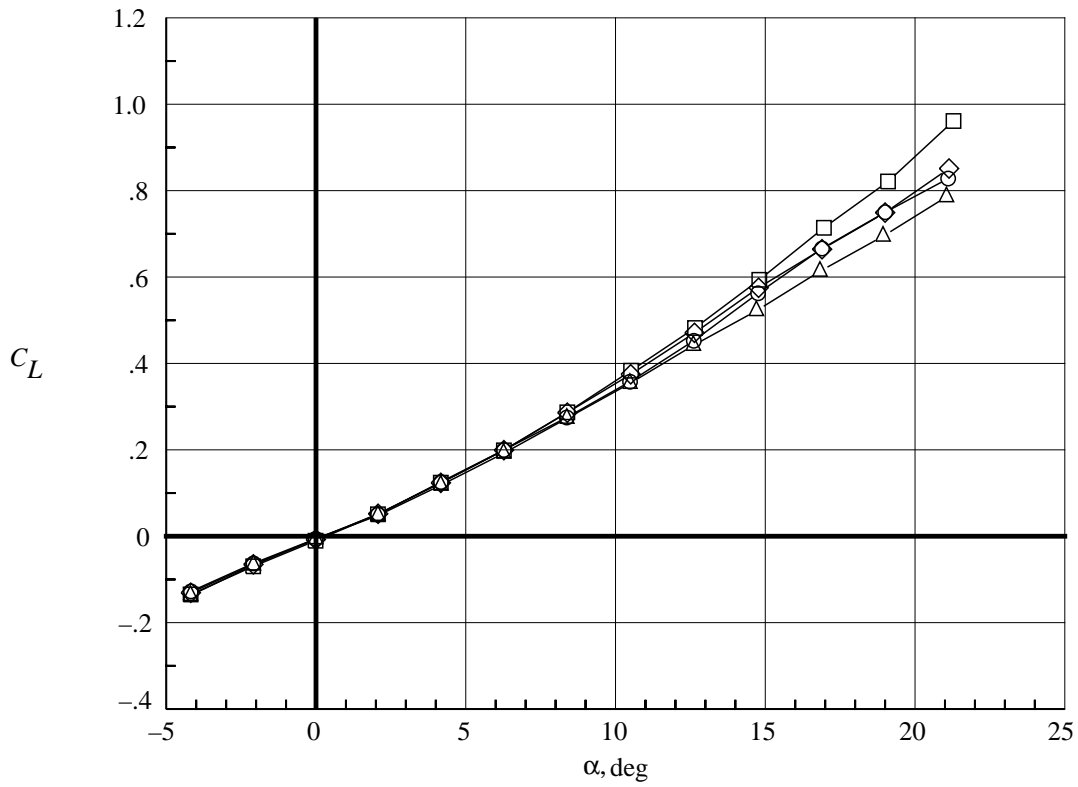
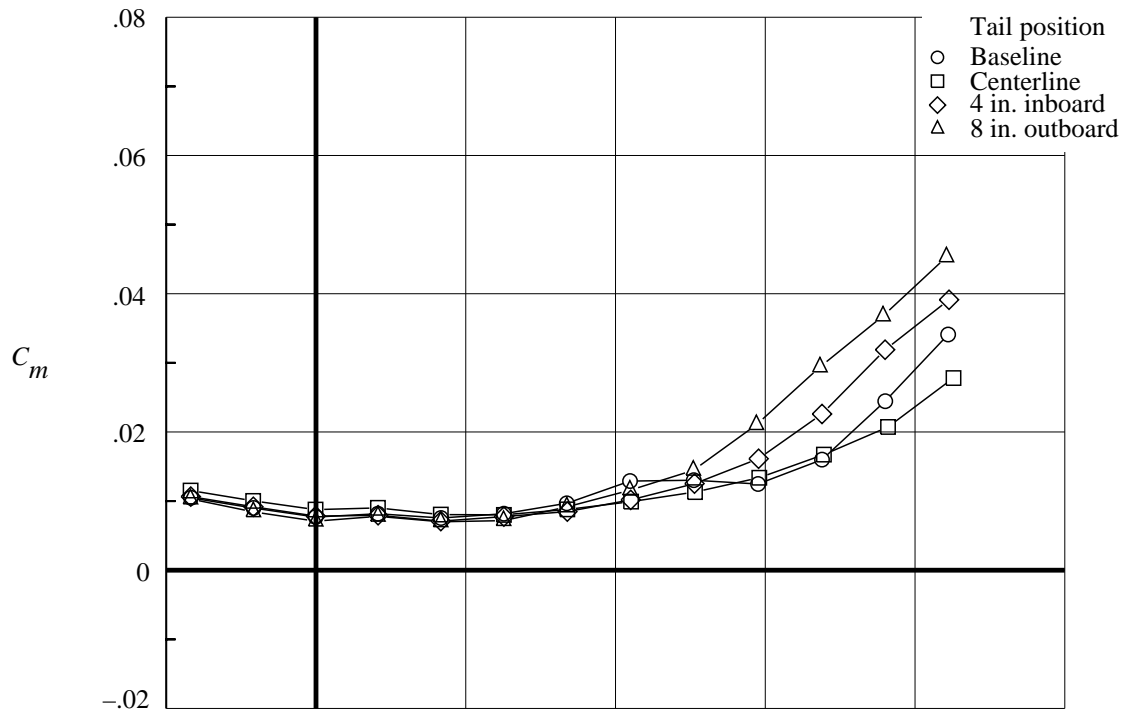
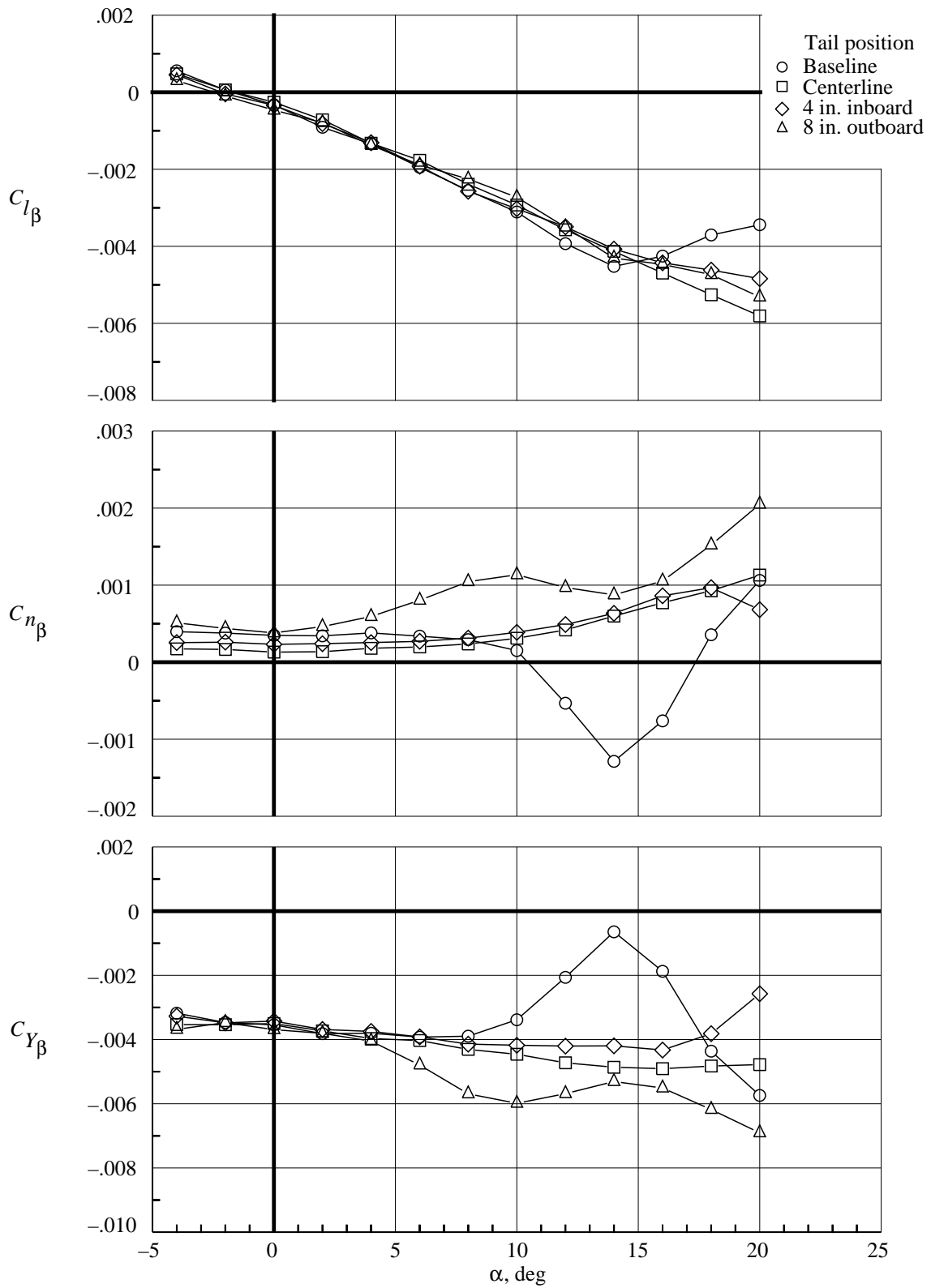


Figure 9. Crosswind landing-control requirements. $\alpha = 10^\circ$, $V_{app} = 151$ knots.



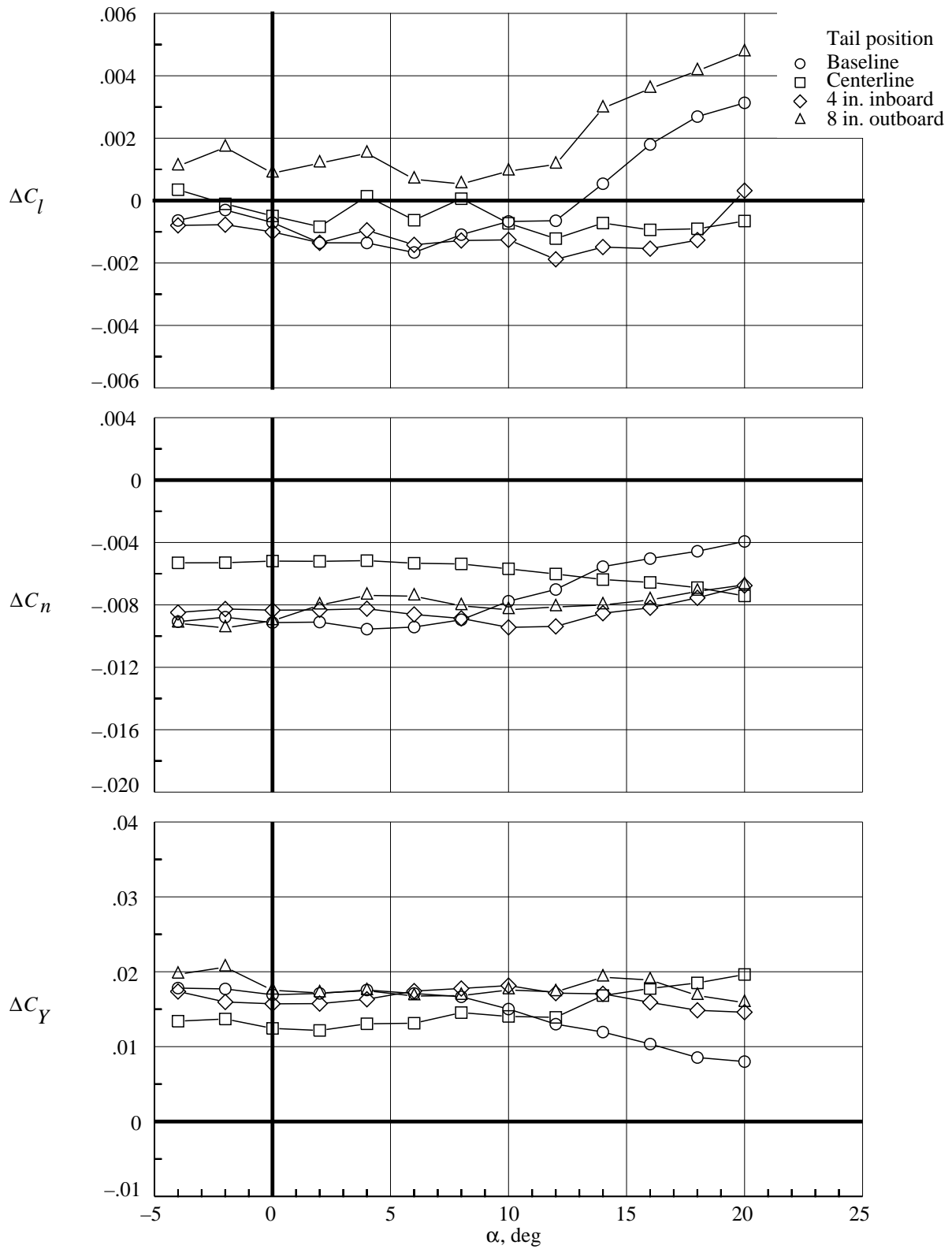
(a) Longitudinal characteristics.

Figure 10. Effect of vertical tail location.



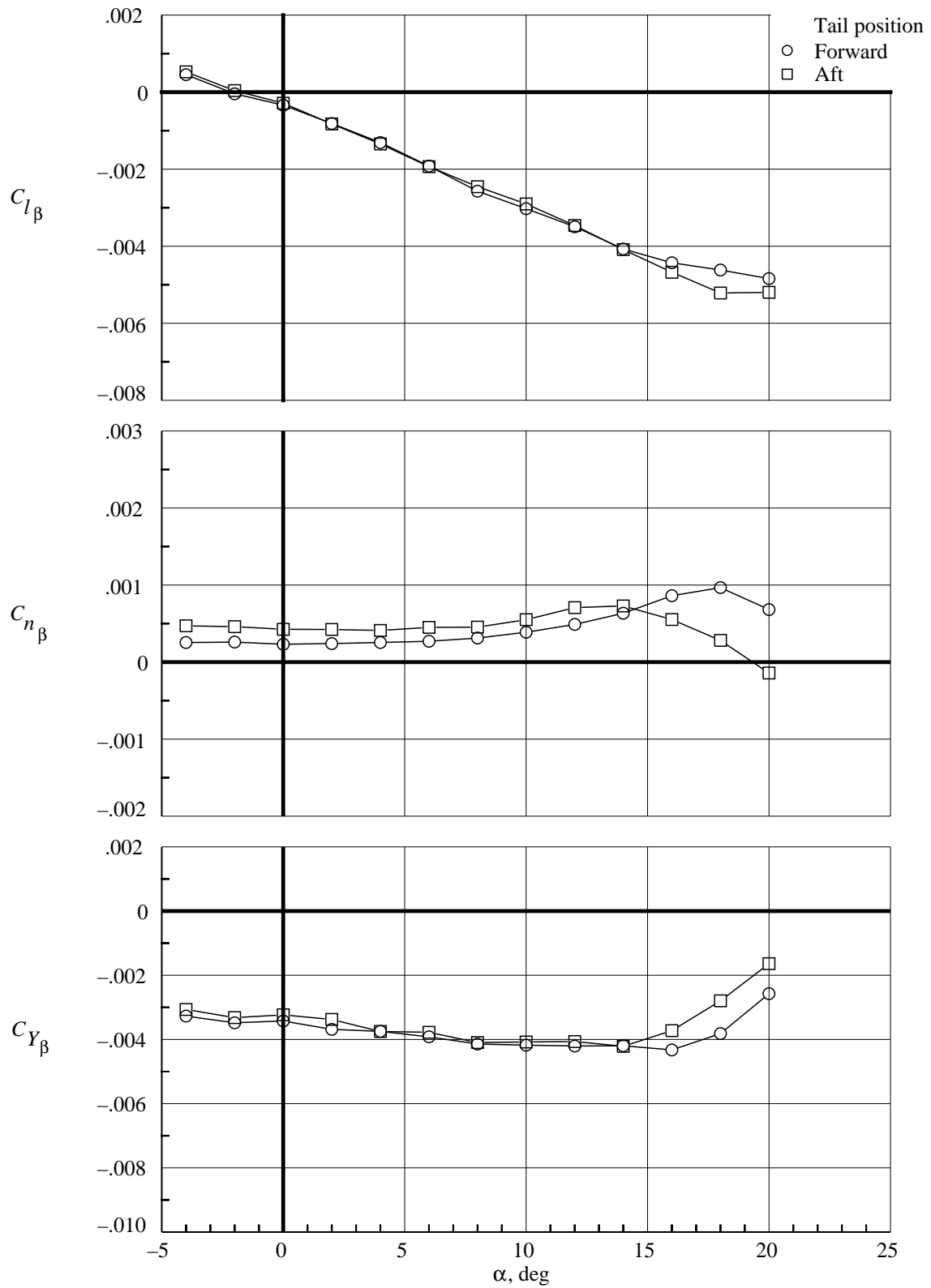
(b) Lateral-directional characteristics.

Figure 10. Continued.



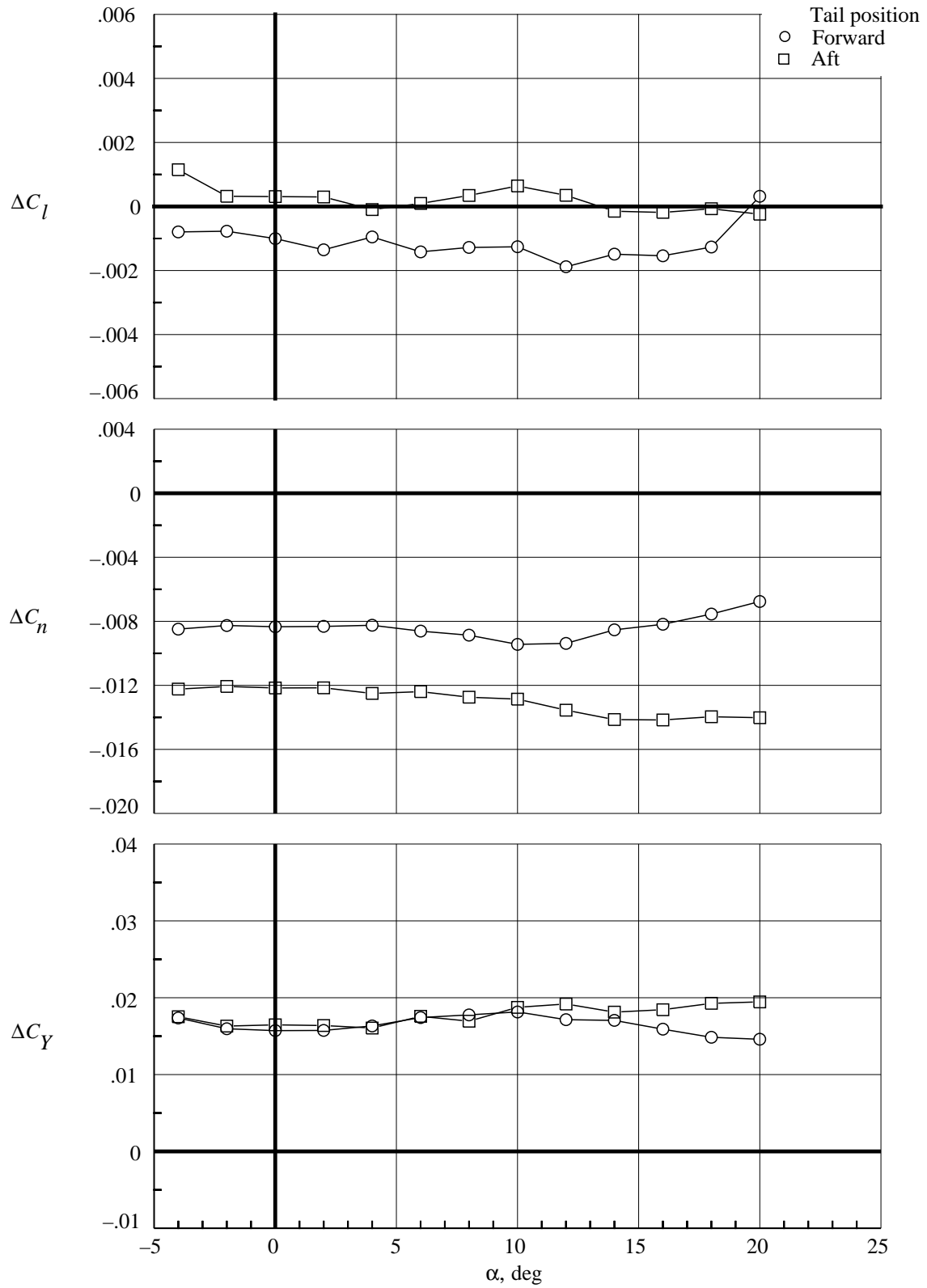
(c) Rudder effectiveness. $\delta_r = 25^\circ/25^\circ$.

Figure 10. Concluded.



(a) Lateral-directional characteristics.

Figure 11. Effect of vertical tail longitudinal position.



(b) Rudder effectiveness. $\delta_r = 25^\circ/25^\circ$.

Figure 11. Concluded.

REPORT DOCUMENTATION PAGE

Form Approved
OMB No. 0704-0188

Public reporting burden for this collection of information is estimated to average 1 hour per response, including the time for reviewing instructions, searching existing data sources, gathering and maintaining the data needed, and completing and reviewing the collection of information. Send comments regarding this burden estimate or any other aspect of this collection of information, including suggestions for reducing this burden, to Washington Headquarters Services, Directorate for Information Operations and Reports, 1215 Jefferson Davis Highway, Suite 1204, Arlington, VA 22202-4302, and to the Office of Management and Budget, Paperwork Reduction Project (0704-0188), Washington, DC 20503.

1. AGENCY USE ONLY <i>(Leave blank)</i>	2. REPORT DATE May 1997	3. REPORT TYPE AND DATES COVERED Technical Memorandum	
4. TITLE AND SUBTITLE Evaluation of the Low-Speed Stability and Control Characteristics of a Mach 5.5 Waverider Concept		5. FUNDING NUMBERS WU 505-70-69-01	
6. AUTHOR(S) David E. Hahne			
7. PERFORMING ORGANIZATION NAME(S) AND ADDRESS(ES) NASA Langley Research Center Hampton, VA 23681-0001		8. PERFORMING ORGANIZATION REPORT NUMBER L-17581	
9. SPONSORING/MONITORING AGENCY NAME(S) AND ADDRESS(ES) National Aeronautics and Space Administration Washington, DC 20546-0001		10. SPONSORING/MONITORING AGENCY REPORT NUMBER NASA TM-4756	
11. SUPPLEMENTARY NOTES			
12a. DISTRIBUTION/AVAILABILITY STATEMENT Unclassified-Unlimited Subject Category 08 Availability: NASA CASI (301) 621-0390		12b. DISTRIBUTION CODE	
13. ABSTRACT <i>(Maximum 200 words)</i> Static force and moment tests of a 0.062-scale model of a hypersonic vehicle study concept known as the LoFLYTE™ configuration were conducted in the Langley 12-Foot Low-Speed Tunnel. These tests looked primarily at the low-speed static stability and control characteristics of this configuration. Data were obtained over an angle-of-attack range of -5° to 22° at sideslip angles that ranged between -10° and 10°. The tiperons were sized to provide enough pitch control to trim the vehicle up to $\alpha = 16^\circ$ with no more than 10° of surface deflection and data obtained in this test showed that 10° of tiperon deflection was nearly sufficient to trim the configuration up to the desired angle of attack. Because of the pitching-moment characteristics of the LoFLYTE™ configuration, there is a reasonably high level of unpowered trimmed lift at nominal takeoff and approach to landing that should allow for acceptable takeoff and landing speeds for this vehicle. Initial evaluation of the directional stability characteristics of this configuration showed a significant instability between $\alpha = 10^\circ$ and about $\alpha = 18^\circ$. This test determined that the cause of this instability was the interaction of the wing leading-edge vortex with the vertical tails. Moving the vertical tails either inboard or outboard from the baseline location eliminated this unfavorable interaction.			
14. SUBJECT TERMS Low speed; Waverider; Stability and control; Vortical flows; LoFLYTE™		15. NUMBER OF PAGES 24	
		16. PRICE CODE A03	
17. SECURITY CLASSIFICATION OF REPORT Unclassified	18. SECURITY CLASSIFICATION OF THIS PAGE Unclassified	19. SECURITY CLASSIFICATION OF ABSTRACT Unclassified	20. LIMITATION OF ABSTRACT